# Oxidative degradation of polyvinyl alcohol by the photochemically enhanced Fenton reaction

Lecheng Lei [a], Xijun Hu [a], Po Lock Yue [a], Stefan H. Bossmann [b], Sabine Göb [b], André M. Braun [b,*]

[a] Department of Chemical Engineering, Hong Kong University of Science and Technology, Clear Water Bay, Kowloon, Hong Kong, China
[b] Lehrstuhl für Umweltmesstechnik, Engler-Bunte-Institut, Universität Karlsruhe, 76128 Karlsruhe, Germany

## Abstract

The effective degradation of polyvinyl alcohol (PVA) was achieved by the application of the photochemically enhanced Fenton reaction. This 'Advanced Oxidation Process' was studied in a batch reactor ($V = 0.75$ l) using a mercury medium pressure light source. The accuracy of the DOC measurements in function of irradiation and reaction time was remarkably enhanced by the addition of a reduction and precipitation agent, consisting of an aqueous solution of $Na_3PO_4$, $Na_2SO_3$ and KI. Effective oxidation was observed when employing low iron(II) concentrations of approximately 1 equivalent of iron(II) per 20 PVA-units ($C_2H_4O$) and a stoichiometric amount of $H_2O_2$ with respect to the PVA-units to be oxidized.    © 1998 Elsevier Science S.A. All rights reserved.

Keywords: Photochemically enhanced Fenton reaction; Advanced oxidation; Oxidative degradation; Environmental pollutants

## 1. Introduction

The release of polyvinyl alcohol from industrial plants, especially in waste water discharged from desizing processes in the textile industry, causes many ecological problems which still need to be solved. These highly polluted waste waters contain up to 10 g dissolved organic carbon (DOC) per liter of waste water causing high Chemical Oxygen Demands (COD) [1]. The oxidative degradation activity of microorganisms in municipal or industrial waste water treatment facilities is usually limited due to the fact that PVA is very difficult to be degraded biologically without specially adapted bacteria strains [2]. Furthermore, PVA enhances the mobilization of heavy metals from the sediments of stream, lakes and oceans [3]. Therefore, methods for the removal of PVA from waste waters, either by mineralization or by chemical transformations, which may also lead to a substantially decreased COD, need to be found.

In recent years, photochemically initiated degradation processes, referred to as 'Advanced Oxidation Processes' (AOP), have been proposed for the treatment of ground, surface and waste waters containing biocidal or non-biodegradable organic compounds [4,5]. As PVA is not readily

biodegradable, its interference with conventional biological treatment methods points to the necessity of an abiotic oxidative pretreatment before its release into biological treatment facilities.

AOP's are most often initiated by hydroxyl radicals which may be generated by various methods (such as UV-C photolysis of hydrogen peroxide, UV photolysis of aqueous solutions of ozone or its reaction with hydrogen peroxide, $TiO_2$ photocatalysis, vacuum ultraviolet (VUV) photolysis of water) [4,6]. Among AOP's, the classic Fenton reaction [7–9] and especially the photochemically enhanced Fenton reaction is considered the most encouraging for the remediation of highly contaminated waste waters. A wide range of successful studies and applications has been reported [10–20], including the successful treatment of industrial waste waters on a large pilot scale (500 l) by the photochemically enhanced Fenton reaction [21].

Recently, Bossmann et al. reported a new evidence for the formation of the ferryl-ion ($Fe_{aq}^{4+}$), instead of the hydroxyl radical, as intermediate of the photochemically enhanced Fenton reaction during the degradation of 2,4-xylidine [22]. The mechanistic scheme of the combination of the thermal and of the photochemically enhanced Fenton reactions is presented in Scheme 1 and consists of the three steps enumerated below.

* Corresponding author. Tel.: +49-721-608-2557; fax: +49-721-608-6240
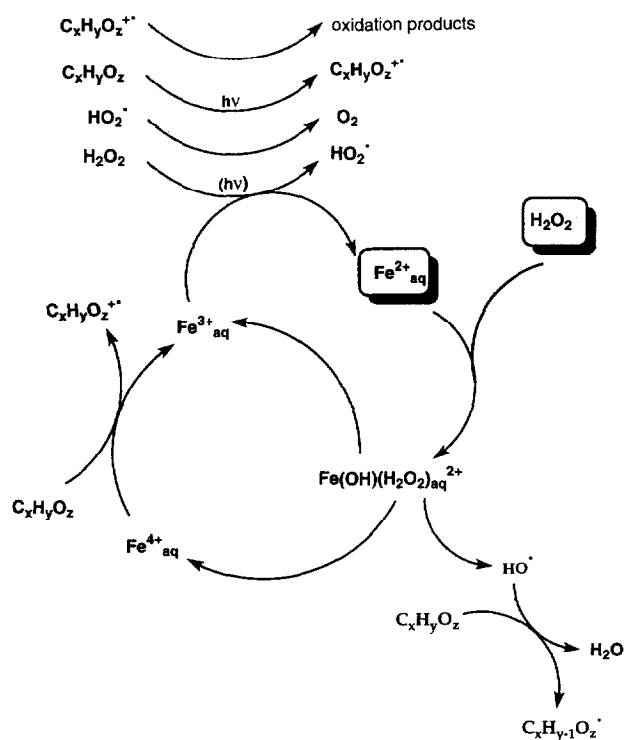
Scheme 1. Mechanistic scheme of reactions involved in the thermal and in the photochemically enhanced Fenton reaction.

1) In aqueous solutions of pH values of 2.5 to 4.5 containing low iron(II) concentrations, $[Fe(OH)(H_2O)_5]^+$ (abbreviated as $Fe_{aq}^{2+}$) is the prevailing chemical species. Upon addition of $H_2O_2$, exchange between iron(II) coordinated $H_2O$ and $H_2O_2$ proceeds under diffusion control (Eq. (1)).

$[Fe(OH)(H_2O)_5]^+$

$$+H_2O_2 \xrightarrow{k_1=2\times10^9 \, s^{-1}} [Fe(OH)(H_2O_2)(H_2O)_4]^+$$

$+H_2O$

(1)
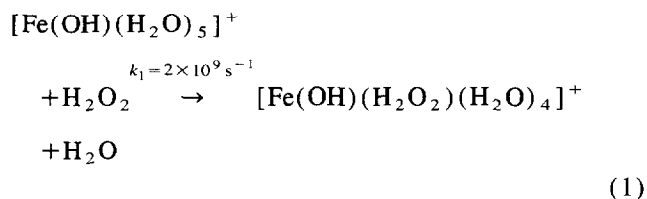
2) After the formation of the hydrated iron(II)–$H_2O_2$ precursor complex (1), an innersphere two-electron transfer reaction occurs (2). This reaction is relatively slow at ambient temperature ($k_2=60$–$80 \, 1 \, mol^{-1} \, s^{-1}$ [23]). The intermediate complex formed is most likely $[Fe(OH)_3(H_2O)_3]^+$ ($Fe_{aq}^{4+}$). The redox potential of the corresponding redox couple $Fe_{aq}^{3+}/Fe_{aq}^{4+}$ has been estimated to be $+1.6\pm0.2$ V (vs. SHE) at a pH of 4.

$[Fe(OH)(H_2O_2)(H_2O)_4]^+$

(2)

$$\xrightarrow{k_2} [Fe(OH)_3(H_2O)_3]^+ + H_2O$$
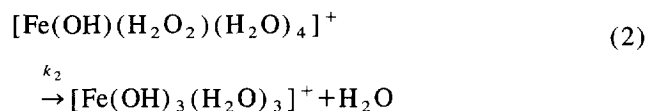
The decay of $Fe_{aq}^{4+}$ in aqueous solution at pH values of 3 to 7 and in the absence of electron donors, such as dissolved organic matter and $H_2O_2$, follows a first-order kinetics with a rate constant of approximately $2 \, s^{-1}$ [24]. Therefore, fast electron transfer reactions between dissolved organic

(macro)molecules (3) possessing oxidation potentials lower than $+1.6\pm0.2$ V (vs. SHE) and $Fe_{aq}^{4+}$ are feasible.
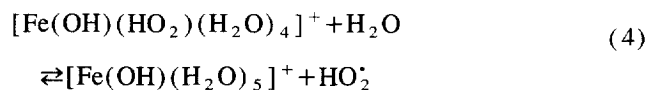
$[Fe(OH)_3(H_2O)_3]^+ + C_xH_yO_z + H_3O^+$

(3)

$$\rightarrow [Fe(OH)(H_2O)_5]^{2+} + C_xH_yO_z^{+\bullet} + H_2O$$
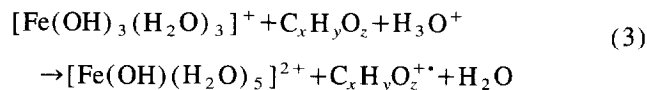
$[Fe(OH)(H_2O)_5]^{2+}$ will be abbreviated as $Fe_{aq}^{3+}$. Oxidative degradation of PVA may, hence, be expected as long as complex formation between iron(II) and $H_2O_2$ is not obstructed.
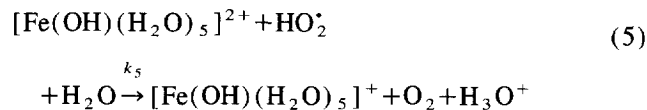
3) The recycling of iron(II) in the (photochemically enhanced) Fenton reaction proceeds according to the following thermal (and photochemical) reactions.

3a) Thermal reduction of $Fe_{aq}^{3+}$ by $H_2O_2$:

This reaction may be described by three consecutive steps: the first step consists of the formation of a hydrated iron(III)–$H_2O_2$ complex ($[Fe(OH)(HO_2)(H_2O)_4^+]$, which is in equilibrium with $Fe_{aq}^{2+} + HO_2\cdot$ ($k_4=0.020 \, 1 \, mol^{-1} \, s^{-1}$ and $k_{-4}=1.2\times10^6 \, 1 \, mol^{-1} \, s^{-1}$) [25].

$[Fe(OH)(HO_2)(H_2O)_4]^+ + H_2O$

(4)

$$\rightleftharpoons [Fe(OH)(H_2O)_5]^+ + HO_2^\bullet$$

Subsequently, a diffusion-controlled irreversible outersphere electron transfer reaction between a second $Fe_{aq}^{3+}$ complex and the hydroperoxyl radical ($HO_2\cdot$) occurs, regenerating a second $Fe_{aq}^{2+}$ ($k_5=2.88\times10^4 \, 1 \, mol^{-1} \, s^{-1}$ [25]).

$[Fe(OH)(H_2O)_5]^{2+} + HO_2^\bullet$

(5)

$$\xrightarrow{k_5} +H_2O \rightarrow [Fe(OH)(H_2O)_5]^+ + O_2 + H_3O^+$$

3b) Photochemical reduction of electronically excited iron(III) by $H_2O_2$:

The thermal reaction (4) may be photochemically accelerated. We determined an apparent quantum yield ($\Phi_{Fe}^{2+}$) of 0.33 for the combined reactions (4), (5) and (6) using mercury medium pressure lamps (Heraeus TQ 150 and Phillips HPK 125) for the electronic excitation of iron(III) [26].

$[Fe(OH)(HO_2)(H_2O)_4]^{+*}$

(6)

$$\xrightarrow{k_6} +H_2O \rightarrow [Fe(OH)(H_2O)_5]^+ + HO_2^\bullet$$
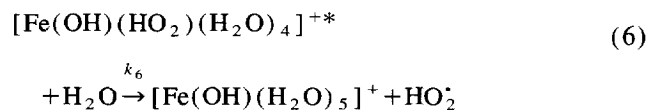
3c) Photochemical reduction of electronically excited iron(III) by dissolved organic matter:

Instead of $H_2O_2$, dissolved organic (macro)molecules may reduce dissolved iron(III) via electron transfer mechanism. The classic ferrioxalate actinometry [26], where oxalate serves as ligand for iron(III) ($\Phi_{Fe^{2+}}=1.24$ ($\lambda_{exc}=254$ nm)), is the best known example for this type of reaction. However, various classes of molecules, such as aromatic amines and phenols, are known to react with similar quantum yields ($0.8<\Phi_{Fe^{2+}}>1.25$, depending on reaction conditions).

It is noteworthy that the photooxidation of water by electronically excited $Fe^{3+}_{aq}^*$ ($\Phi_{Fe^{2+}}=0.2\pm0.05$ [27]) does not play any significant role in the mechanistic scheme of the photochemically excited Fenton reaction. It may only com-

pete with the other reduction pathways for iron(III) at very low concentrations of dissolved organic matter [22].

Based on this mechanistic hypothesis, the effect of the complexation of iron(II) and especially of iron(III) by the PVA macromolecules on the degradation efficiency is of great scientific interest. In this respect, PVA does not only serve as a model compound for many iron(III)-chelating macromolecules, but may in general be used as a probe to investigate the reaction mechanism of oxidative polymer degradation which is of great importance to many industrial applications.

## 2. Experimental

### 2.1. Chemicals

$FeSO_4 \times 7$ $H_2$, $(Fe)_2(SO_4)_3 \times 11$ $H_2O$, $H_2O_2$, $H_2SO_4$, $Na_3PO_4$, $H_3PO_4$, $KMnO_4$, $Na_2SO_3$, KI, oxalic acid, acetaldehyde, ethanol, 1,10-phenanthroline, acetonitrile and acetic acid were supplied by Merck. PVA (3 well defined PVA-standards, $M_w = 15,000$, 49,000 and 100,000) was bought from Sigma. All chemicals were ACS grade. Water was of bidistilled quality (UHQ II).

UV/VIS-spectra were recorded using an Hewlett-Packard 5800(II) diode array spectrophotometer. A Metrohm (E 512) pH-analyzer was employed. $H_2O_2$ was analyzed by classic $KMnO_4$ titration [28].

### 2.2. Ferrioxalate-actinometry [26]

The radiant powers ($P_e$ [W]) of the medium pressure mercury lamps (Heraeus, TQ 150, quartz filter, electrical power consumption: 150 W, and Phillips HPK 125, quartz filter, electrical power consumption 125 W) employed in this work were determined by using ferrioxalate actinometry ($[Fe_{aq}^{3+}] = 2.40 \times 10^{-2}$ mol $l^{-1}$, [oxalic acid] $= 2.40 \times 10^{-2}$ mol $l^{-1}$). The method is based on the photochemical reduction of iron(III) to iron(II) and oxidation of oxalic acid to $CO_2$. The photochemically generated $Fe_{aq}^{2+}$ has been measured quantitatively by using the VIS absorption of iron(II)(tris-1,10-phenanthroline) ($[Fe(phen)_3]^{2+}$, $\varepsilon_{510}$ $_{nm} = 11,100 \, l \, mol^{-1} \, cm^{-1}$) which is formed from $Fe^{2+}{}_{aq}$ and 1,10-phenanthroline in 0.50 mol $l^{-1}$ of aqueous acetic acid [26]. Under experimental standard conditions of the ferrioxalate actinometry, $2.75 \times 10^{-5}$ mol $l^{-1}$ $s^{-1}$ (TQ 150) and $2.30 \times 10^{-5}$ mol $l^{-1}$ $s^{-1}$ of $Fe_{aq}^{2+}$ (HPK 125) were formed. From these data and using the relative emission spectrum of the mercury medium pressure lamps (Fig. 1), values for $P_e$ of $45.6 \pm 1.2$ W (TQ 150) and $38.2 \pm 0.9$ W (HPK 125) have been calculated (7).

$$P_e = \frac{n_{Fe^{2+}}}{t \sum_\lambda \left( \frac{S_{e,\lambda}}{E_{ph,\lambda}} (1 - 10^{-A_\lambda}) \right) \Phi_\lambda} \qquad (7)$$
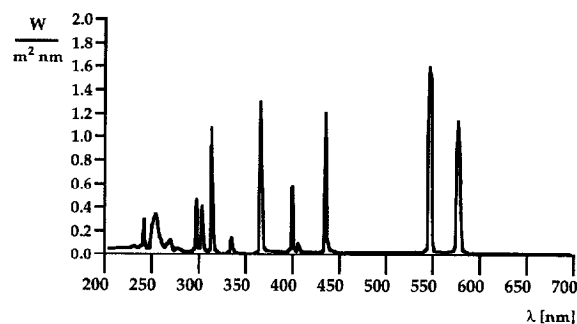


Fig. 1. Spectral distribution of the medium pressure mercury lamp (Heraeus, TQ 150) used for polychromatic irradiation experiments.

where $n_{Fe^{2+}}$: number of $Fe_{aq}^{2+}$ ions formed during the irradiation time $t$, $t$: irradiation time [s], $S_{e,\lambda}$: relative spectral distribution of the emission of the light source (Fig. 1), $E_{ph\lambda}$: energy of a photon of wavelength $\lambda$ [J], $A_\lambda$: average absorbance of the actinometric solution at wavelength $\lambda$ during irradiation, $\Phi_\lambda$: quantum yield of the chemical actinometer at wavelength $\lambda$ [26].

### 2.3. Thermal and photochemically enhanced fenton reactions

All photolysis experiments were carried out in a batch reactor (Fig. 2). It consists of a reservoir ($V = 0.55$ l), a flow-through annular photoreactor ($V = 0.15$ l) equipped with a mercury medium pressure lamp (TQ 150 or HPK 125). The solution was recirculated ($0.25 \pm 0.02$ l min$^{-1}$) by means of a pump (Bender and Hobein, masterflex, easy-load 75-118-00). Solutions were continuously purged (in the reservoir) by compressed air or nitrogen (actinometry). All photolysis experiments were performed for a duration of 120 min. The temperature of the solutions was kept at $40 \pm 2°C$.

The total volume of the solutions to be photolyzed was 0.50 l. The initial concentration of PVA was $8.325 \times 10^{-3}$



Fig. 2. Photochemical batch reactor employed in all irradiation experiments.

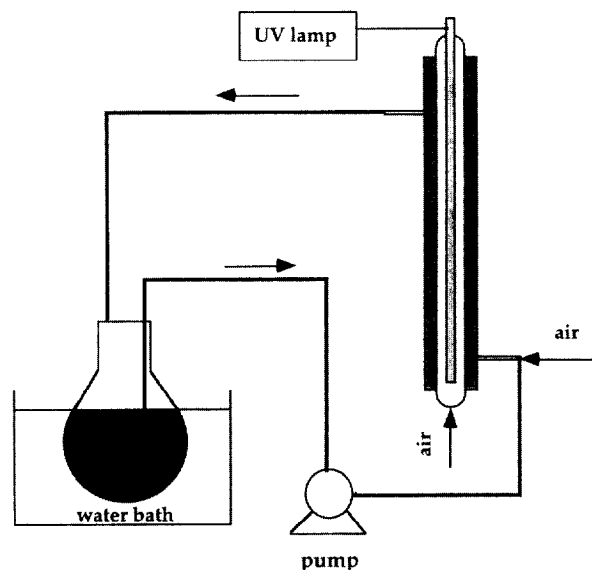equiv. $l^{-1}$ of VA-units ($C_2H_4O$) or 200 mg C $l^{-1}$ (366.7 mg $l^{-1}$ of PVA). The standard concentration of iron(II) was $4.16 \times 10^{-4}$ mol $l^{-1}$ resulting in a molar ratio of iron(II) to PVA-units of 1:20. The total amount of iron(II) was dissolved in the PVA solution before $H_2O_2$ was added. The stoichiometric amount of $H_2O_2$ required to totally oxidize the PVA was $3.33 \times 10^{-2}$ mol $l^{-1}$ (100%) as calculated according to Eq. (8).

$$\text{(structure)} + 5n\ H_2O_2 \longrightarrow 2n\ CO_2 + 7n\ H_2O \qquad (8)$$

$$C_2H_4O + 2.5\ O_2 \longrightarrow 2\ CO_2 + 2\ H_2O$$

The pH has been adjusted to the initial value of 4.0 using $H_2SO_4$. No significant dependence of the reaction rates of PVA degradation on the pH value of the reaction mixture has been observed between pH = 2.0 and 4.0. Analyses were performed immediately after the samples were taken and filtered using Nylon Luer-Lock membrane filters (Roth, $0.22 \times 10^{-4}$ m).

### 2.4. Treatment of the analysis samples prior to DOC and HPLC measurements

$2.0 \times 10^{-3}$ l of a reduction and precipitation agent, composed of 0.10 mol $l^{-1}$ of $Na_3PO_4$, 0.10 mol $l^{-1}$ of KI and 0.10 mol $l^{-1}$ of $Na_2SO_3$, was added to a volume of $3.0 \times 10^{-3}$ l taken from the batch reactor at various irradiation times. This procedure led to a complete reduction of the residual $H_2O_2$ as well as to the removal of most of the iron(II/III) by precipitation. The precipitate was removed by filtration using Nylon Luer-Lock membrane filters.

### 2.5. DOC Analysis

The analysis of the DOC (dissolved organic carbon) has been carried out using a Dohrmann DC-190 TOC (total organic carbon) analyzer ($T = 680°C$) from Rosemount Analytical. Calibration has been performed using PVA ($M_w = 15,000$, 49,000 and 100,000), oxalic acid and potassium hydrophthalate (KHP). All calibration samples fall on a single straight line.

### 2.6. HPLC measurements

The detection of possible low-molecular weight intermediates of the PVA degradation by means of the photochemically enhanced Fenton reaction, such as oxalic acid, acetic acid, acetaldehyde or ethanol, was performed using an HP 1090 Series II Liquid Chromatograph, equipped with a diode-array detection system (DAD). A LiChrospher-100 RP18 column ($l = 125$ mm, diameter = 4 mm, particle size = 5 μm) and an identical precolumn were employed. The precolumn removed higher weight intermediates ($M_w > 2000$). As eluent, a mixture of 0.05 mol $l^{-1}$ of triethylamine/$H_3PO_4$ (pH = 7.0, 95% v/v) and acetonitrile (5% v/v) was chosen.

However, no low molecular weight intermediates were detected at all (detection limit: $1.0 \times 10^{-7}$ mol $l^{-1}$).

## 3. Results and discussion

### 3.1. Comparison of UV/VIS spectra

Fig. 3 shows the UV/VIS spectra of aqueous PVA, iron(II) and iron(III) solutions as well as of solutions of the complexes of PVA with iron(II). The original PVA and $Fe_{aq}^{2+}$ solutions show very little absorption limited to the UV spectral region. The $Fe_{aq}^{3+}$ solution has a significant absorption in the region of 200 to 330 nm extending into the VIS spectral region. PVA may form complexes with ferrous ions which also show absorption in the UV spectral region. PVA-ferric ion complexes effectively absorb light up to 500 nm.

UV/VIS spectra of the reaction mixture during the thermal and the photochemically enhanced Fenton reactions are shown in Figs. 4 and 5, respectively. The UV/VIS spectrum of the initial solution compares quite well with that of the PVA-ferrous ion complexes (Fig. 3). The spectral characteristics change and become similar to those of the PVA-ferric ion complexes when $H_2O_2$ is added. PVA being degraded in this process, the amount of PVA-ferric ion complexes is reduced, and, consequently, absorption in the region of 260 to 400 nm is diminished. The remaining absorption in the spectral region of 200 to 260 nm may be caused by complex formation of ferric ions and PVA fragments which are further degraded at a slower rate. Comparing the results of Figs. 4 and 5, it is evident that the use of light significantly enhances both the rate and the final level of degradation. This is explained by the photochemical enhancement of the transi-



Fig. 3. UV-spectra ($d = 1$ cm) of aqueous PVA, $Fe^{2+}$, $Fe^{3+}$ solution and their mixtures with PVA as used in the photolysis experiments.
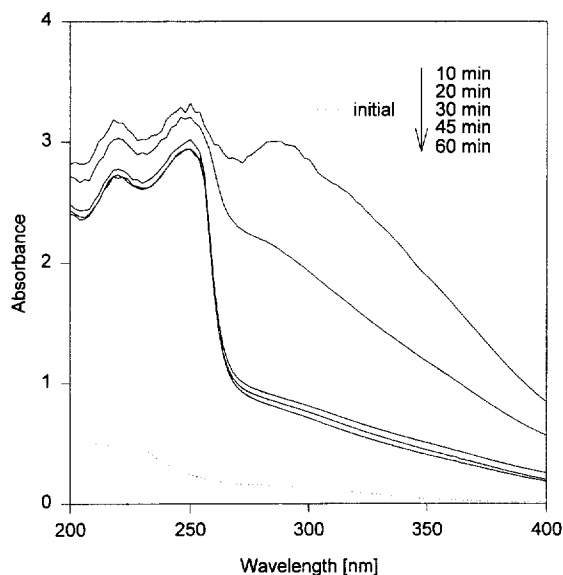
Fig. 4. UV-spectra ($d = 1$ cm) during the thermal Fenton reaction in the presence of PVA, performed under standard conditions (100% stoichiometric amount of $H_2O_2$, PVA of 200 mg C $l^{-1}$, a ratio of 1 mol of $Fe^{2+}$ to 20 mol of PVA units).
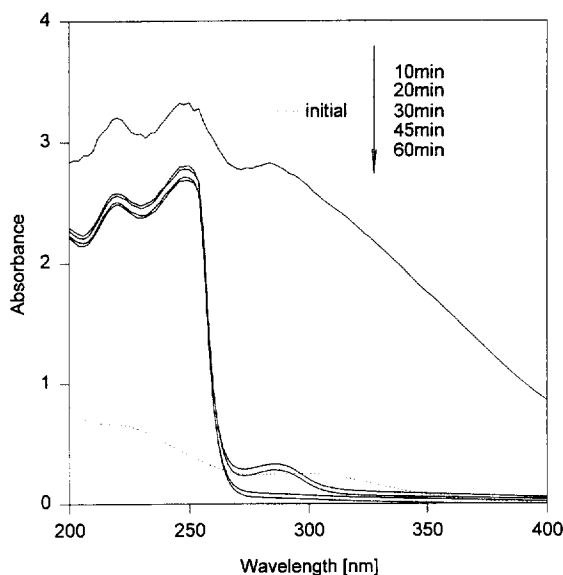


Fig. 5. UV-spectra ($d = 1$ cm) during the photochemically enhanced Fenton reaction in the presence of PVA, performed under standard conditions.

tion frequency of ferric to ferrous ions, hence, accelerating the ferrous ion catalyzed (thermal) reaction.

### 3.2. Effect of the reductive and precipitation agent

The measurement of the PVA degradation as a function of oxidation conditions depends strongly on the ability of the experimentalist to stop the oxidation reaction at a chosen reaction time. For such investigations, it is absolutely necessary to prevent further oxidation by the thermal Fenton route after having taken a sample from the reactor. In spite of being significantly slower than the photochemically enhanced Fenton reaction, the thermal Fenton reaction will
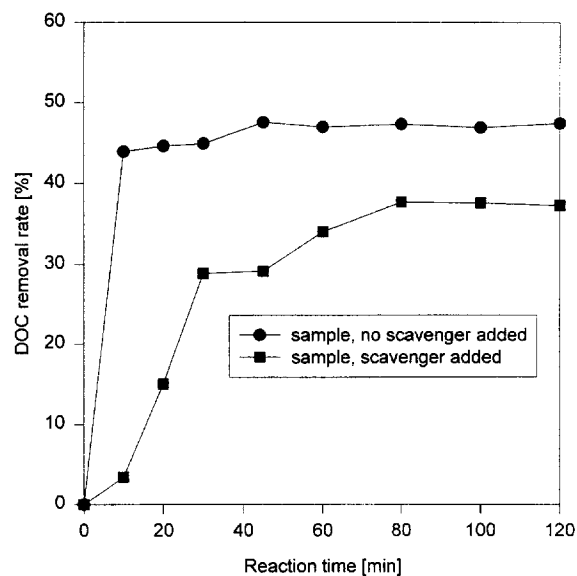


Fig. 6. Effect of the reduction and precipitation agent on the result of the DOC analysis during the thermal Fenton reaction in the presence of PVA.

continue as long as $H_2O_2$ prevails in the reaction system, even at lower temperatures (refrigerator). Therefore, a reductive and precipitation agent, consisting 0.10 mol $l^{-1}$ of $Na_3PO_4$, 0.10 mol $l^{-1}$ of KI and 0.10 mol $l^{-1}$ of $Na_2SO_3$ was added in order to reduce all residual $H_2O_2$. Furthermore, ferric and ferrous ions precipitate in the presence of basic phosphate solution and may be removed from the solution by filtration. Fig. 6 shows the effect of the reductive and precipitation agent on the apparent DOC removal of PVA ($M_w = 15,000$) in function of reaction time. The experiments were performed by adding 100% of the stoichiometric amount of $H_2O_2$ at $t_0$. The curve referred to as 'no scavenger added' means that prior to analysis the samples were stored without further treatment in a refrigerator at 4°C for 16 h. It is obvious that further oxidation of PVA occurred during the storage period, even at lower temperatures, and that significant experimental errors may emerge if the reaction cannot be stopped immediately after the analysis sample was taken.

### 3.3. Effect of PVA polymer size

The reaction mechanism of PVA degradation during the photochemically enhanced Fenton reaction may be investigated by examining the dependence of the rate of mineralization on the molecular weight of PVA. Therefore, we choose three different monodisperse PVA model polymers and compared their reaction behavior under exactly the same experimental conditions.

The results of the DOC analysis of samples taken at different reaction times during thermal and photochemical experiments are shown in Fig. 7. No low molecular weight intermediates, such as oxalic acid, acetic acid, acetaldehyde or ethanol could be detected by HPLC, the threshold of detection (DOC) being approximately 1 mg C $l^{-1}$. Within 30 min of reaction time, $90 \pm 4\%$ of the DOC of all three monodis-
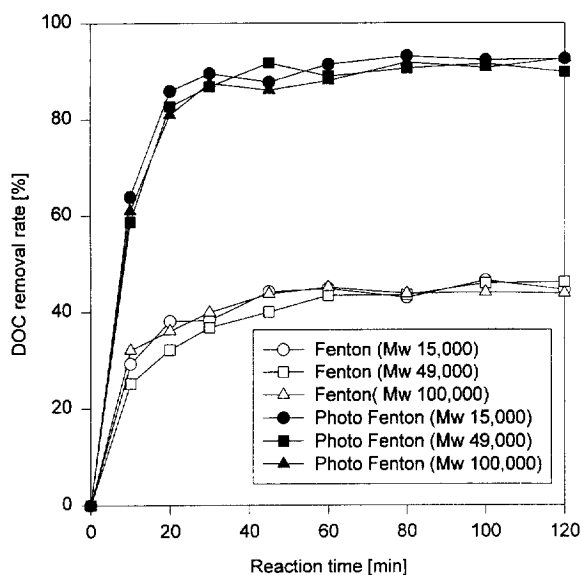
Fig. 7. Degradation of PVA of three different molecular weights by the thermal and the photochemically enhanced Fenton reaction.
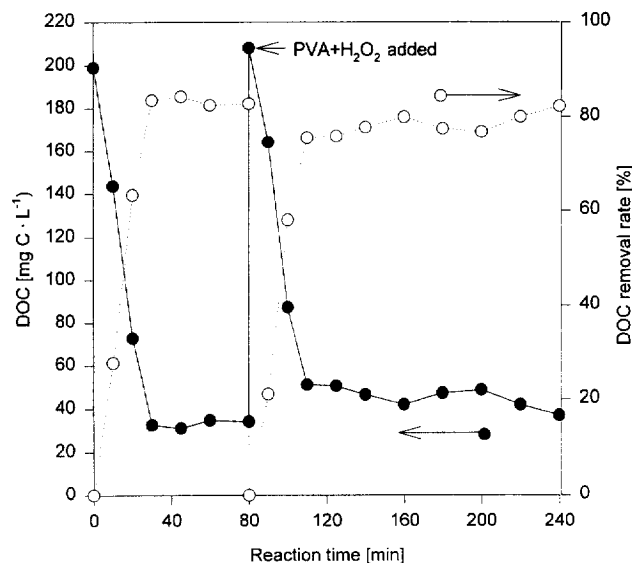


Fig. 8. PVA degradation by the photochemically enhanced Fenton reaction under standard conditions, $M_w = 49,000$. After 80 min the same amounts of PVA and $H_2O_2$ were added for a second time.

perse PVA model polymers was mineralized in the photochemically enhanced Fenton reaction. The thermal Fenton reaction was slower to reach a smaller final DOC removal rate of $40 \pm 5\%$.

Apparent reaction rate constants of the initial DOC removal (mineralization) might be determined by fitting the curves shown in Fig. 7 on the basis of a first order kinetic model or by taking the corresponding slopes for reaction times of up to 10 min (pseudo zero order kinetic model). As we may already deduce from Fig. 7, the result of these calculations reveal two distinct apparent rate constants for each set of experiment (thermal vs. photochemically enhanced Fenton reaction) with a deviation of maximum $\pm 9.1\%$ for both thermal and photochemical experiments. The ratio of the two apparent rate constants yields the factor of the enhancement due to the photochemical ferrous ion regeneration (vide supra) of $5.6 \pm 20\%$.

### 3.4. Double addition of PVA

The appearance of a plateau (90% DOC conversion rate) during the photochemically enhanced Fenton oxidation of PVA raised some doubts about the application of this 'Advanced Oxidation Process' in continuous flow reaction systems as well as in case of higher PVA concentrations ($> 5000$ ppm [C]). A pragmatic test to investigate the fate of the remaining organic carbon consists in adding a defined amount of PVA and the corresponding stoichiometric amount of $H_2O_2$, once the reaction has reached the plateau region. Fig. 8 shows the evolution of the DOC and the corresponding DOC removal rate during a photochemical experiment in which 200 mg C $l^{-1}$ of PVA ($M_w = 49,000$) and a stoichiometric amount of $H_2O_2$ were added again after 80 min of irradiation time.

The results represented in Fig. 8 show that the degradation of PVA by the photochemically enhanced Fenton reaction is equally fast for both PVA oxidation cycles. In fact, the slopes calculated in accord with a pseudo zero order kinetic model for the first 30 min after each PVA and $H_2O_2$ are the same within limits of error of 9%.

Again, a second DOC plateau region was reached after 30 min of irradiation time. The DOC removal rate reached $79 \pm 3\%$, hence 5% less than measured for the first DOC plateau. This is a promising result for the development of a continuous process on a pilot scale. However, in parallel, the presence of iron(II) and iron(III) complexes with organic ions of low thermal (after total consumption of added $H_2O_2$) and photochemical reactivity has to be reinvestigated in order to find a complete mass balance of the organic carbon. From the data shown, the residual DOC of 42 mg C $l^{-1}$ could be totally complexed by $4.16 \times 10^{-1}$ mol $l^{-1}$ of iron ions yielding iron complexes with 8 equivalents of carbon per iron ion.

### 3.5. Effect of the iron(II)/PVA ratio

Based on our working hypothesis that iron ion would be predominantly complexed by PVA, the rate of DOC removal should be effected by the ratio of the concentrations of iron(II) and PVA. Fig. 9 summarizes the results which were obtained by the variation of the iron(II) concentration in the presence of 200 mg C $l^{-1}$ of PVA ($M_w = 49,000$). The initial PVA degradation proceeds fastest at the highest iron(II) concentration corresponding to a ratio of 1 equivalent of iron(II) per 5 PVA-units. However, the plateau region is reached at a DOC removal rate of $75 \pm 2\%$ which is significantly higher than at the lower iron(II) concentrations investigated ($84 \pm 3\%$).

Although, higher rates of degradation at higher iron(II)/PVA ratios may be expected, the increase of refractory matter
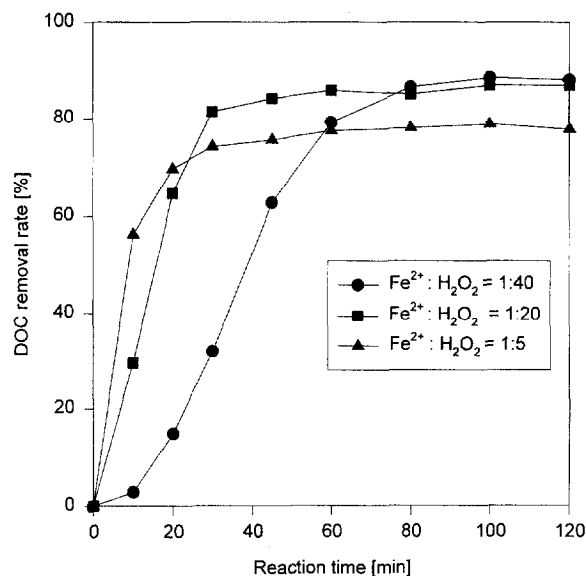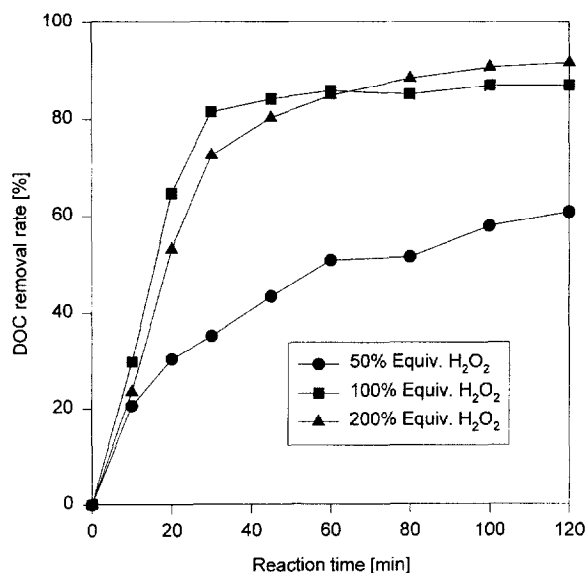
Fig. 9. PVA degradation by the photochemically enhanced Fenton reaction under standard conditions, $M_w = 49,000$ and different iron(II) concentrations.

formed during the photochemically enhanced Fenton degradation of PVA and depending on the total iron ion concentration is a strong argument in favor of an important complex formation between iron(II) / (III) and PVA and its intermediate products of degradation.

### 3.6. Effect of the $H_2O_2$/PVA ratio

In analogy to the variation of the amount of iron(II) added, the $H_2O_2$ concentration was also varied. The results are shown in Fig. 10. It is interesting to note that an increase of the $H_2O_2$ concentration does not result in a significant effect on the initial rate of degradation. Again, this finding corroborates with earlier development and modeling work [29].



Fig. 10. PVA degradation by the photochemically enhanced Fenton reaction under standard conditions, $M_w = 49,000$ and different $H_2O_2$ concentrations.

For conditions of a ratio of at least 1 mol of $H_2O_2$ to 1 PVA-unit, the experiments result in a plateau region at $85 \pm 4\%$ DOC removal rate. Although, the results could be interpreted that the residual DOC might be mineralized employing large excesses of $H_2O_2$, a twofold stoichiometric amount of $H_2O_2$ might be already beyond economical limits for such a process at technical level.
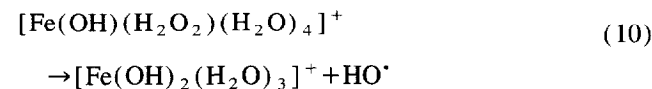
### 4. Conclusion

The oxidative degradation of PVA by means of the photochemically enhanced Fenton reaction has shown promising results at a laboratory scale. It has been demonstrated that at a ratio of 1 equivalent iron(II) per 20 mol of PVA-units and employing a stoichiometric $H_2O_2$/PVA-unit ratio, approx. 90% of the initial DOC may be mineralized within 30 min under the experimental conditions applied. The factor of the photochemical enhancement was 5.6 depending primarily on the absorbed photon rate and the ratio between irradiated and total volume of the photochemical reactor [29]. Further development of this process will lead to shorter irradiation times even for waste waters containing higher amounts of DOC.

Beside the pragmatic view of applied photochemistry, the results of this investigation permit to establish a first mechanistic hypothesis.

The classic mechanism of the iron(II) accelerated $H_2O_2$ decomposition is based on a simple redox mechanism in which iron(II) is oxidized to iron(III) and $H_2O_2$ reduced to hydroxide ion generating at the same time a hydroxyl radical (9) [9].

$$Fe^{2+} + H_2O_2 \rightarrow Fe^{3+} + HO^- + HO^{\bullet} \tag{9}$$
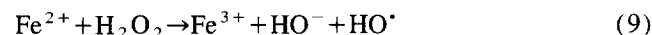
In analogy to Eq. (2), the reaction might be explained by

$$[Fe(OH)(H_2O_2)(H_2O)_4]^+ \tag{10}$$

$$\rightarrow [Fe(OH)_2(H_2O)_3]^+ + HO^{\bullet}$$

Consequently, hydroxyl radicals would attack PVA by hydrogen abstraction (11), hence initiating its oxidative degradation via peroxyl radicals (12) [30].
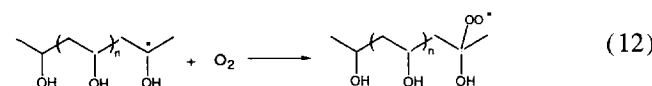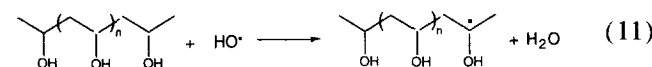


So far, the kinetic results do not permit to differentiate between the mechanisms involving iron(III)/PVA complexes and hydroxyl radicals, respectively. There is, however, at least some evidence, as shown below, for a mechanism which does not involve hydroxyl radicals.

1) No low molecular weight intermediates of the oxidative degradation of PVA have been detected by HPLC. These findings differ significantly from the results of the Fenton reaction in the presence of phenols, aromatic amines or aliphatic alcohols and acids [22], where oxalic acid prevails as process intermediate.

2) The DOC removal rate at sub-stoichiometric $H_2O_2$ concentrations in function of irradiation time (Fig. 10) does not corroborate with a scheme involving reactions (1) and (10). On the basis of such a scheme, we would suggest that this curve remains linear (predominantly pseudo zero order) for up to 80% of the $H_2O_2$ consumption.

In contrast, the early deviation of this curve may be explained by the complexation of iron with PVA and intermediate products of PVA degradation preventing $H_2O_2$ to approach and complex with the metal centers. This latter reaction seems to be the rate determining step of this process.

3) The same hypothesis might be valid to explain the plateaus of DOC removal and, in particular, their dependence on the iron(II/III) concentration (Fig. 9).

4) If arguments 1) to 3) hold, the fast predominant pseudo zero order removal of more than half of the initial DOC suggests that PVA is a better complexing agent than the intermediate products of degradation.

Our first series of experiments provide evidence for a complex formation between PVA and iron(II)/(III) and, consequently, for the oxidation of PVA by intermediate iron(IV)-species formed in the thermal Fenton reaction. Since no low molecular weight intermediates are found, we may assume that $CO_2$ is released as oxidation product.

The reduction of PVA-bound iron(III) to iron(II) is achieved photochemically. The quantum yield of this process is currently under investigation.

## Acknowledgements

## References

[1] L. Lei, G. Chen, J.F. Porter, P.L. Yue, Proceedings of the Third International Conference on Advanced Oxidation Technologies, Columbus, OH, 1996, 27–29.

[2] K. Schluter, Textile auxiliaries—sizing agents, Ullmann's Encyclopedia of Industrial Chem. A26 (1995) 244–253.

[3] A. Ziemann, Forum Staedte-Hygiene 4 (1994) 214–217.

[4] O. Legrini, E. Oliveros, A.M. Braun, Chem. Rev. 93 (1993) 671–698.

[5] D.F. Ollis, H. Al-Ekabi, (Eds.), Photocatalytic Purification and Treatment of Water and Air, Elsevier, Amsterdam, 1993.

[6] G.V. Buxton, C.L. Greenstock, W.P. Helman, A.B. Ross, J. Phys. Chem. Ref. Data 17 (1988) 513–532.

[7] H.J.H. Fenton, J. Chem. Soc. 65 (1894) 899.

[8] H.J.H. Fenton, J. Chem. Soc. Trans. 75 (1899) 1–11.

[9] C. Walling, Acc. Chem. Res. 8 (1975) 125–131.

[10] A.E. Cahill, H. Taube, J. Am. Chem. Soc. 74 (1952) 2312.

[11] E.A. Pasek, D.K. Straub, Inorg. Chem. 11 (1972) 259–266.

[12] W. Feuerstein, E. Gilbert, S.H. Eberle, Vom Wasser 56 (1981) 35–54.

[13] M. Barbeni, C. Minero, E. Pelizzetti, E. Borgarello, N. Serpone, Chemosphere 16 (1987) 2225–2237.

[14] D.L. Sedlak, A.W. Andren, Environ. Sci. Technol. 25 (1991) 777–782.

[15] E. Lipczynska-Kochany, Chemosphere 22 (1991) 529–536.

[16] G. Ruppert, R. Bauer, G. Heisler, J. Photochem. Photobiol. A: Chem. 73 (1993) 75–78.

[17] S. Andrianirinaharivelo, G. Mailhot, M. Bolte, Solar Energy Materials and Solar Cells 38 (1995) 459–474.

[18] A. Safarzadeh-Amiri, J.R. Bolton, S.R. Cater, J. Advanced Oxid. Technol. 1 (1996) 18–26.

[19] J.J. Pignatello, G. Chapa, Environ. Toxicol. Chem. 13 (1994) 423–427.

[20] Y. Sun, J.J. Pignatello, Environ. Sci. Technol. 27 (1993) 304–310.

[21] E. Oliveros, O. Legrini, M. Hohl, T. Müller, A.M. Braun, Chem. Eng. Proc. 3 (1997) 397–405.

[22] S.H. Bossmann, E. Oliveros, S. Göb, S. Siegwart, E.P. Dahlen, L.P. Payawan Jr., M. Straub, M. Wörner, A.M. Braun, J. Phys. Chem., 1998, in print.

[23] C. Walling, K. Amarnath, J. Am. Chem. Soc. 104 (1982) 1185–1189.

[24] M.L. Kremer, G. Stein, Trans. Faraday Soc. 55 (1959) 560–595.

[25] C. Walling, A. Goosen, J. Am. Chem. Soc. 95 (1973) 2987–2991.

[26] A.M. Braun, M.-T. Maurette, E. Oliveros, Photochemical Technology, Wiley, New York, Chichester, 1991.

[27] B.C. Faust, J. Hoigne, J. Atm. Environ. 24 (1990) 79–89.

[28] G. Jander, E. Blasius, E. Einführung in das anorganisch-chemische Praktikum; Hirzel, Stuttgart, 1984.

[29] A.M. Braun, L. Jakob, E. Oliveros, C.A. Oller do Nascimento, in: D.H. Volman, G.S. Hammond, D.C. Neckers (Eds.), Adv. Photochem., Wiley, New York, 1993, 235–313.

[30] C. von Sonntag, H.-P. Schuchmann, Angew. Chem. 103 (1991) 1255–1279.